RSC Pharmaceutics

ROYAL SOCIETY OF CHEMISTRY

PAPER

View Article Online
View Journal | View Issue

Cite this: *RSC Pharm.*, 2026, **3**, 552

Polymeric nano-in-microparticles for pulmonary delivery of remdesivir against SARS-CoV-2

Alison Tatiana Madrid Sani,[a,b] Brenno da Cunha Lima,[d] Beatriz Moreira Rodrigues,[d] Michelle Alvares Sarcinelli,[c] Marcelo Henrique da Cunha Chaves,[c] Helvécio Vinícius Antunes Rocha,[c] Natália Neto Pereira Cerize,[a] Maria Helena Ambrosio Zanin,[a] Juliana Terzi Maricato,[d] Valker Araujo Feitosa*[b] and Carlota de Oliveira Rangel-Yagui *[b]

Received 30th September 2025,
Accepted 18th January 2026

DOI: 10.1039/d5pm00269a

rsc.li/RSCPharma

The COVID-19 pandemic underscored the urgent need for advanced drug delivery systems to enhance the safety and efficacy of existing antiviral therapies. This study presents an inhalable powder formulation of remdesivir (RDV) using polymeric nano-in-microparticles for pulmonary administration. RDV was nanoencapsulated in a polycaprolactone (PCL) matrix *via* emulsion–diffusion–solvent evaporation and stabilized with DPPC and Pluronic F127, resulting in nanoparticles (RDV-PCL-NP) of 184 ± 11 nm and 87% encapsulation efficiency. Cytotoxicity assays in Vero E6 cells confirmed the RDV-PCL-NP safety at therapeutic concentrations, with a marked reduction in the SARS-CoV-2 viral load at 5 μM RDV. The nanoparticles were spray dried with lactose, yielding a dry powder (RDV-PCL-MP) with 63% process yield. Physicochemical characterization (SEM, FTIR, DRX, DSC/TGA, laser diffraction) confirmed uniform particle size and stability (1–5 μm) of the RDV-PCL-MP inhalable powder. *In vitro* lung deposition studies showed 40% fine fraction and 39% respirable fraction. These findings support the potential of RDV-loaded nano-in-microparticles as a scalable pulmonary delivery platform to improve COVID-19 treatment.

1. Introduction

The COVID-19 outbreak caused by the SARS-CoV-2 coronavirus has posed a challenge to global health, prompting continued efforts to develop effective prevention and treatment strategies. Among several therapeutic options, remdesivir (RDV) was the first drug approved by the FDA for the treatment of COVID-19 and is currently administered intravenously to hospitalised patients.[1] RDV readily crosses cell membranes and is converted to its active metabolite GS-443902, which inhibits viral RNA polymerase activity and stops viral RNA replication.[2] Its use has been extended to non-hospitalized patients with mild to moderate COVID-19 who are at high risk of progression to severe disease due to comorbidities such as diabetes or chronic obstructive pulmonary disease (COPD).[3]

In addition to RDV, oral antivirals such as molnupiravir and paxlovid® (commercial association of nirmatrelvir and ritonavir) have been approved for emergency use in adult patients at an increased risk of severe COVID-19. However, the Food and Drug Administration (FDA) and the Brazilian Health Regulatory Agency (ANVISA) recommended RDV as the preferred antiviral agent.[4] Challenges associated with the clinical use of RDV are its low oral bioavailability and hydrophobic nature, and it requires dissolution in sulfobutyl ether-beta-cyclodextrin (SBCD) for intravenous administration over at least two hours.[5] This prolonged administration compromises patient convenience and introduces risks associated with systemic exposure to RDV and SBCD, including hepatic and renal complications.[6] Clinical data suggest adverse event rates of 70%–74% during the 5–10 day treatment period, with severe adverse events leading to early discontinuation in 21%–34% of cases.[7] In addition, intravenous administration may result in suboptimal pulmonary drug concentrations insufficient to inhibit viral replication in the lung, primarily due to rapid systemic metabolism to GS-441524, a metabolite unable to cross the cell membrane.[5]

In the last four years, several studies have been published focusing on the nanoencapsulation of RDV, most of them based on liposomes.[8] One study reported the encapsulation of RDV in polymeric nanoparticles of PCL/PLGA-PEG.[9] However, the reported study is limited to the concept of nano-in-microparticles

[a]*Bionanomanufacturing Center, Technological Research Institute, São Paulo, Brazil*
[b]*Department of Biochemical and Pharmaceutical Technology, School of Pharmaceutical Sciences, University of São Paulo, São Paulo, SP, Brazil. E-mail: valker@usp.br, corangel@usp.br*
[c]*Laboratory of Micro and Nanotechnology, Oswaldo Cruz Foundation, Rio de Janeiro, Brazil*
[d]*Department of Microbiology, Immunology and Parasitology, Federal University of São Paulo, São Paulo, Brazil*

and has not progressed to powder formulations. It does not include antiviral confirmation and aerodynamic characterization.

Pulmonary delivery has therefore emerged as an attractive strategy to overcome these limitations. Inhaled formulations can deliver high local concentrations of RDV directly to the respiratory epithelium, enabling rapid antiviral action while minimizing systemic exposure and bypassing first-pass metabolism and rapid plasma clearance.[10] Compared with nebulization, dry powder inhalers (DPIs) offer several advantages, including superior physical stability, no need for cold-chain storage, reduced contamination risk, improved patient convenience, and increased suitability for outpatient and home-based treatment. These advantages make DPIs particularly valuable in pandemic situations where decentralized therapy and rapid drug administration are critical.

In this work, we have developed a powder formulation of nano-in-microparticles containing RDV. Biocompatible excipients like PCL, DPPC, Pluronic® F127 and lactose were used, capable of stabilizing the drug, enhancing dispersibility, and suitable for a sustained-release. This approach provides a versatile and scalable strategy for encapsulating not only RDV, but also other hydrophobic drugs. In particular, it addresses first-pass hepatic metabolism and could increase the RDV concentration in the lungs, providing a targeted therapeutic option for patients with COVID-19.

2. Experimental

2.1 Preparation of nanoparticles containing RDV (RDV-PCL-NP)

Polycaprolactone (PCL 10 kDa, Sigma Aldrich, USA), soybean lecithin S75® (phospholipid rich in dipalmitoylphosphatidylcholine – DPPC, Lipoid, Germany), and remdesivir (Ambeed, USA) were dissolved in 5 mL of ethyl acetate at molar ratios of 0.06, 0.19 and 0.75 of RDV : PCL : DPPC. The solution was placed in an ultrasonic bath (P30 kHz, Elma, Gottlieb, Germany) at 50 °C for 25 min for complete homogenization. The organic phase was slowly added to an aqueous solution of 500 μg mL^{-1} of Pluronic® F127 (PEO_{99}-PPO_{65}-PEO_{99}, Sigma Aldrich, USA) and emulsified for 5 min at 14 000 rpm in an Ultra-turrax® (IKA, Germany). The system was diluted with 50 mL of deionized water and evaporated in a rotary evaporator R-215 (Büchi, Switzerland) at 45 mbar to remove the organic solvent, resulting in RDV-PCL-NP. Blank nanoparticles (PCL-NP) were also prepared as a control.

2.2 Evaluation of the RDV-PCL-NP dispersion stability

PCL-NP and RDV-PCL-NP formulations were stored in a refrigerator (4 °C) and analyzed periodically (at least once a week) by dynamic light scattering (DLS) using a NanoPlus Zeta/Nano Analyzer (Micrometrics, USA). For analysis, samples were diluted at 1 : 50 in purified water. Particle size and polydispersity index (PDI) results are presented as the mean of three independent measurements (n = 3) plus standard deviation.

2.3 Evaluation of the RDV-PCL-NP zeta potential

The surface charge of the nanoparticles was estimated by measuring the zeta potential using a Malvern Zetasizer Nano ZS (NanoPlus, Particulate Systems). PCL-NP and RDV-PCL-NP formulations were diluted in water (refractive index 1.33), and measurements were performed at 25 °C with 10 runs per analysis. Formulations were analyzed in triplicate and results are reported as mean zeta potential values using the NanoPlus software.

2.4 Determination of remdesivir loading and encapsulation efficiency

Drug loading (DL) and encapsulation efficiency (EE, %) were determined by high performance liquid chromatography. Analytical HPCL was conducted on a Shimadzu LC-20AD (Kyoto, Japan) with a C18 Supelco Ascentidi column (4.6 mm, 5 μm) at a flow rate of 1.5 mL min^{-1} (injection volume 20 μL). The mobile phase consisted of 20 mM KH_2PO_4 (pH 7.5) and acetonitrile in the proportion of 50 : 50 (v/v). The RDV concentration was determined at a wavelength of 247 nm based on a standard curve. DL was calculated using the following eqn (1):

$$\mathrm{DL}\,(\%) = \frac{\text{mass of encapsulated drug}}{\text{total mass of particles}} \times 100 \quad (1)$$

The EE (%) was calculated using eqn (2).[11]

$$\mathrm{EE}\,(\%) = \frac{L_a}{L_t} \times 100 \quad (2)$$

where L_a is defined as the total mass of RDV encapsulated and L_t is expressed as the initial RDV mass that has been added to the system.

2.5 Cytotoxicity assays

Vero E6 cells were cultivated in Eagle's Minimum Essential Medium (MEM; Gibco, USA) with the addition of 10% fetal bovine serum (FBS; Gibco, USA). The cells were seeded in 48-well plates at a density of 100 000 cells per well and maintained at 37 °C in a humidified atmosphere with 5% CO_2. Following 24 h of incubation, the medium was removed and the cells were treated with 100 μL of fresh medium containing varying concentrations of free RDV and RDV-PCL-NP. The cytotoxic potential of RDV and RDV-PCL-NP formulations was evaluated 48 h post-treatment by measuring the release of lactate dehydrogenase (LDH), a cytosolic enzyme released into the extracellular medium upon plasma membrane damage, serving as an indicator of cell membrane integrity. For the positive control, cells in two wells were exposed to 1% Triton X-100 (Bio-Rad Laboratories, USA) to induce complete cytotoxicity. After 48 h, the interstitial fluid was harvested from the designated wells and transferred into labelled tubes for analysis. The LDH concentration in the resultant supernatant was then measured using the CyQUANT™ LDH cytotoxicity assay kit (Thermo Fisher Scientific, USA). The untreated culture medium was used as a negative control. The calculation of the levels of cytotoxicity was performed in relation to the absorbances of the positive control, which was used as the 100% reference point for the calculation of the levels of cytotoxicity.

2.6 Antiviral efficacy

A SARS-CoV-2 viral isolate from the original Wuhan strain (EPI_ISL_413016, provided by the Albert Einstein Hospital, São Paulo, Brazil) was used to infect Vero E6 cells, in accordance with the protocol described by Hoffmann *et al.* (2020). Viral titration was performed using the Plaque Forming Unit (PFU per mL) method, which quantifies infectious viral particles by determining the number of plaques formed in a cell culture.[12] Concurrently, molecular detection was conducted through RT-qPCR, as recommended for the detection of SARS-CoV-2.[13] PFU per mL values were correlated with Cycle Threshold (Ct) values from RT-qPCR experiments to calculate the Multiplicity of Infection (MOI). After a thorough analysis of the available data, a MOI of 1.0 was selected as the most appropriate for simulating conditions of high viral load in the assays.

2.7 Viral load quantification

The extraction of viral RNA from the culture media of infected Vero E6 cells was accomplished by means of the QIAamp® Viral RNA mini kit (QIAGEN, USA). The quantification of RNA was performed using a NanoDrop™ spectrophotometer (Thermo Fisher Scientific, USA), and reverse transcription was carried out using the AgPath-ID™ One-Step RT-PCR Reagents (Thermo Fisher Scientific, USA) to generate cDNA and enable single-step amplification and detection. Amplifications were performed on the 7500 Real-Time PCR System (Applied Biosystems, USA), with subsequent data analysis conducted using 7500 software v2.3 and Microsoft Excel. The relative gene expression was calculated using the 2-ΔΔCt method. The thermal cycling conditions comprised an initial 50 °C for 2 min, followed by 95 °C for 10 min, and then 40 cycles of 95 °C for 15 s and 60 °C for 1 min. The protocol was concluded with a melting curve analysis. Vero E6 cells (ATCC, no. 1586) were cultured in MEM supplemented with 10% fetal bovine serum (FBS; Gibco, USA) and seeded at a density of 1×10^5 cells per well in 48-well plates. After 24 h of incubation at 37 °C with 5% CO_2, cells were pretreated with 100 μL of medium containing varying concentrations of RDV or RDV-PCL-NP for 1 h. Subsequently, cells were infected with the SARS-CoV-2 isolate (EPI_ISL_413016) at a MOI of 1.0 for 2 h. Following the infection period, the medium containing the formulations and virus was removed, the cells were washed twice with PBS, and fresh medium containing the formulations was added. Cells were maintained under these conditions for 48 h at 37 °C with 5% CO_2.

The quantification of viral RNA in the extracts was conducted by RT-qPCR, using primers and probes that targeted the Rdrp gene. This procedure adhered to the 2019-nCoV RT-qPCR protocol, which was established by the Pasteur Institute. The reaction was performed using the Hot Start Go Taq® mix (Promega, USA) on a 7500 Real-Time PCR System (Applied Biosystems, USA). The quantification of viral RNA copy numbers was performed with the help of a calibration curve generated with synthetic RNA, and the results were visualized using GraphPad Prism 7 (GraphPad Software, USA).

2.8 Preparation of the polymeric nano-in-microparticle powder formulation (RDV-PCL-MP)

Preparation of nano-in-microparticles was previously optimized by our group.[14] Initially, 1% (w/v) of micronized lactose (Lactohale® LH206, DFE Pharma, Germany) was added to the nanoformulations (PCL-NP and RDV-PCL-NP). Then, the systems were placed in a spray-dryer (mini B190, Büchi, Switzerland) filled with a stainless-steel standard fluid nozzle tip of 0.5 mm internal diameter. The drying conditions were fixed at an inlet temperature of 100 °C, an atomizing air flow of 600 L h^{-1}, an aspirator air flow of 70%, and a feed rate of 4.5 mL min^{-1}. After spray drying, the powder formulations were stored within a desiccator at ambient temperature and the process yield was calculated as the % (wt) of the powder collected in relation to the initial total weight of the solids (lactose and nanoparticles).

2.9 Physicochemical characterization of the polymeric nano-in-microparticle powder formulation (RDV-PCL-MP)

The excipients and the microparticles containing or not RDV (RDV-PCL-MP, PCL-MP) were analyzed by field emission electron microscopy (3D-FEG-SEM, Quanta, USA), laser light diffraction (Mastersizer 2000, Malvern, United Kingdom), differential scanning calorimetry (DSC822, Mettler-Toledo, Switzerland), thermogravimetric analysis (TGA/DSC 1 STARe System, Mettler-Toledo, USA), X-ray powder diffraction (X-ray diffractometer, Rigaku, USA), and attenuated total reflectance and Fourier transform infrared spectroscopy (Nicolet Is10 Spectrometer, ThermoFisher, USA) as previously described.[14]

2.10 *In vitro* aerosolization performance

Samples of 25 mg of RDV-PCL-MP previously dispersed with micronized lactose LH206 (1 : 1) were added to hard capsules (size 4, Infinity Pharma, Brazil). Then, the capsules were placed in a dry powder inhaler device (Aerolizer®), perforated once and evaluated regarding the aerosolization performance in a Next Generation Impactor (NGI®, Copley Scientific, United Kingdom) as previously described.[14] The experiment was conducted in quintuplicate (five capsules). The emitted dose ED (%) (eqn (3)) was used to express the percentage of ED based on the total dose (TD) used.[15]

$$\mathrm{ED}\,(\%) = \frac{\mathrm{ED}}{\mathrm{TD}} \times 100\% \tag{3}$$

The fine particle dose (FPD) was defined as the dose deposited on stages 2–7 and the fine particle fraction (FPF%) (eqn (4)) was expressed as the percentage of FPD to ED.

$$\text{Fine particle fraction}\,(\mathrm{FPF}\%) = \frac{\mathrm{FPD}}{\mathrm{ED}} \times 100\% \tag{4}$$

The respirable fraction (RF%) (eqn (5)) was used as the percentage of FPD to total deposited dose (DD) on all impactor stages.

$$\text{Respirable fraction}\,(\mathrm{RF}\%) = \frac{\mathrm{FPD}}{\mathrm{DD}} \times 100\% \tag{5}$$

The Mass Median Aerodynamic Diameter (MMAD) represents the median aerodynamic diameter of the particles in

the aerosol. It was determined based on the cumulative particle size distribution functions obtained from NGI data.

2.11 Statistical analysis

Statistical analysis was performed using OriginPro 8 (OriginLab Corporation, Wellesley, MA, USA). Depending on the dataset, Student's *t*-test or one-way ANOVA followed by Tukey's *post hoc* test was applied. These analyses were used to evaluate cytotoxicity and viral load data for RDV, RDV-PCL-NP, and PCL-NP in Vero E6 cells and SARS-CoV-2-infected cultures.

3 Results and discussion

3.1 Characterization and stability of the nanoparticles

3.1.1 Dynamic light scattering (DLS). The scattering profile of PCL-NP containing or not RDV is presented in Fig. 1a. As can be seen, the blank PCL-NPs presented a mean hydrodynamic diameter of 156 ± 8 nm, while the RDV-PCL-NPs presented a mean hydrodynamic diameter of approximately 184 ± 11 nm. The polydispersity index (PdI) was determined to be 0.081 ± 0.017 and 0.137 ± 0.011, respectively, suggesting homogeneous monodisperse systems.[9] The reduced size and uniform size distribution of the NPs are a result of the emulsification–diffusion–evaporation method, since the proportion of components in the organic phase combined with the application of high shear force (*e.g.*, 14 000 rpm) facilitates the breakdown of droplets into smaller and more consistent sizes.[16] Additionally, the maintenance of an excess aqueous phase has been demonstrated to enhance the solvent diffusion efficiency. Furthermore, conducting the diffusion and evaporation processes at a controlled low temperature (*e.g.* 50 °C) has been shown to support the formation of uniform and stable NPs. These findings underscore the pivotal role of formulation parameters and processing conditions in attaining well-defined NP properties, which are indispensable for stability and potential therapeutic efficacy. Further optimization of polymer/surfactant concentrations, shear speed, and solvent compositions could expand the applicability of this method to a broader range of drug delivery systems, ensuring enhanced performance and targeted delivery.[17]

Significant progress has been made in the encapsulation of antiviral drugs within PCL to enhance their efficacy, bioavailability, controlled release, and site-specific delivery. This is exemplified by the encapsulation of adefovir dipivoxil, ritonavir, oseltamivir, and acyclovir, which have demonstrated substantial improvements in these crucial properties.[18] These examples highlight the potential of PCL as a material for nanoencapsulation of antiviral drugs. As demonstrated in Fig. 1b, the colloidal dispersion (RDV-PCL-NP) preserved the hydrodynamic diameter and narrow monomodal size distribution at 4 °C for a period of up to six months. Although our final goal was to develop a nano-in-micro powder formulation, this results provide the possibility to further investigate the colloidal dispersion for nebulization. Nonetheless, powder formulations are much more stable than liquid ones owing to the reduced water activity.

3.1.2 Zeta potential. The formulations exhibited slightly negative surface charges, with zeta potential values ranging from −4.94 ± 0.10 mV to −5.10 ± 0.12 mV, which falls within the interval of −10 to +10 mV typically associated with near-neutral particles.[13] This mild negative charge may result from partial hydrolysis of PCL, leading to the exposure of acidic groups on the nanoparticle surface. PCL-based nanoparticles frequently display negative zeta potentials when used for antiviral delivery. For instance, tenofovir-loaded PCL nanoparticles showed a zeta potential of −19.1 mV, attributed to surface carboxyl groups,[2] while acyclovir-loaded PCL nanoparticles similarly exhibited negative values and good colloidal stability.

3.1.3 Determination of remdesivir encapsulation efficiency (%EE) by HPLC. The chromatograms of RDV and formulations containing or not RDV (RDV-PCL-NP, PCL-NP) are presented in Fig. 2 and the characteristic peak of RDV was identified at 4.7 min of retention time (Fig. 2a). This peak is also observed

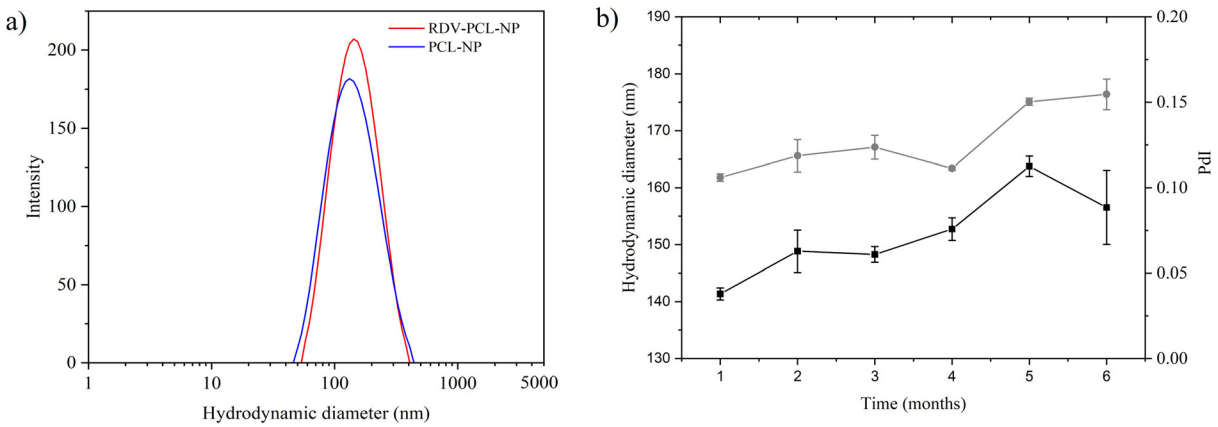

Fig. 1 (a) Hydrodynamic diameter of RDV-PCL-NP and PCL-NP, (b) hydrodynamic diameter (red line) and polydispersity index (black line) of RDV-PCL-NPs during six months of storage at 4 °C based on dynamic light scattering measurements. Results are presented as the mean of three independent measurements (n = 3) plus standard deviation.

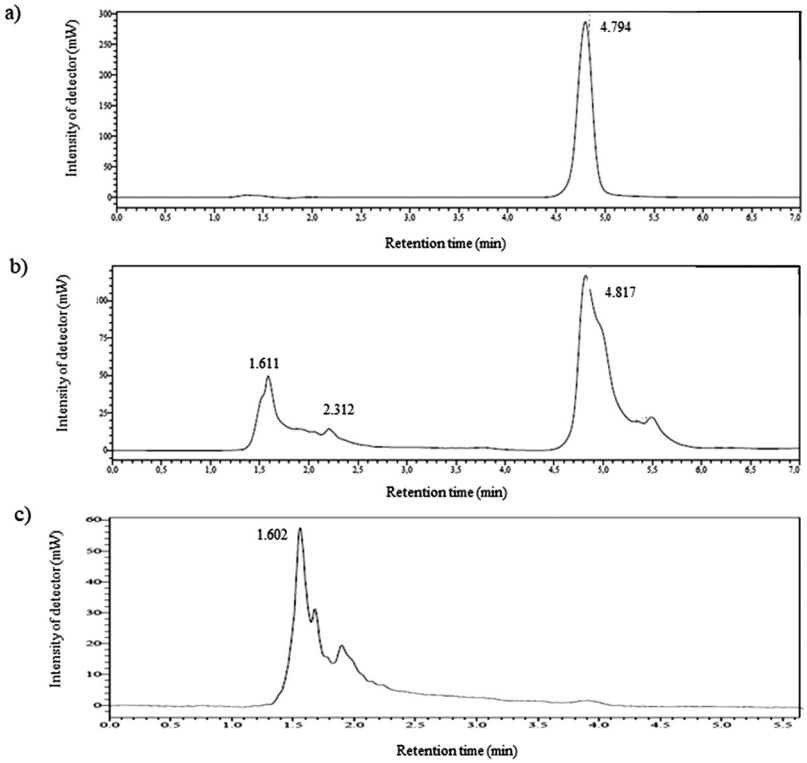

Fig. 2 (a) Chromatogram of RDV, (b) chromatogram of the formulation containing RDV (RDV-PCL-NP) and (c) chromatogram of the blank formulation (PCL-NP).

in RDV-PCL-NP (Fig. 2b), which confirms the successful incorporation of the drug into the formulation. A secondary peak at approximately 1.6 min and smaller peaks between 1.8 and 2.3 min were also observed, likely corresponding to residual materials from the formulation components including PCL, Pluronic F-127, DPPC, and lactose LH206, which were not entirely removed during the centrifugation step prior to HPLC analysis. The RDV peak was not detected in the PCL-NP formulation (Fig. 2c), as expected. However, the presence of a peak at 1.6 min was evident, indicating the presence of residual materials from the excipients used in the formulation.

The encapsulation efficiency of PCL nanoparticles can vary depending on the preparation method. For instance, nanoprecipitation techniques have been shown to result in %EE as high as 90%. Conversely, the emulsification/diffusion/solvent evaporation method typically yields %EE ranging from 50% to 80%, influenced by the ratio of PCL to the drug.[19] In the present study, the RDV-PCL-NP resulted in EE% = 87% and a drug loading (%DL) of 1.74%; our system provided higher EE% when compared to previous studies. Values of %EE of 72% were obtained for the encapsulation of RDV in PLGA/chitosan nanoparticles,[10] whereas %EE = 82% was obtained with bis-MPA hyperbranched dendritic nanocarriers.[20] The RDV : PCL ratio of 1 : 4 provided an optimal polymeric matrix for encapsulation of RDV, while DPPC improved structural stability and increased the %EE. In addition, Pluronic F127, applied as a polymeric surfactant, ensured stability during the emulsification and diffusion processes, thereby inhibiting particle aggregation and yielding uniform particles, which facilitated a high %EE.[21] These results highlight the capability of PCL nanoparticles to effectively encapsulate the hydrophobic RDV, demonstrating the potential of this method to develop efficient drug delivery systems.

3.2 Cytotoxicity assays

The results of free and nanoencapsulated RDV cytotoxicity are presented in Fig. 3 and, as can be seen, no statistically significant differences ($p > 0.05$) were identified in cell viability between the negative control and cells exposed to the formulations at lower drug concentrations (up to 2.5 μM). In contrast, at 5 μM RDV the RDV-PCL-NP presented significantly lower cytotoxicity levels compared to the free drug ($p < 0.01$), indicating that nanoencapsulation effectively mitigates RDV-induced cytotoxicity at higher concentrations. Slight cytotoxicity was observed for the PCL-NPs at higher concentrations, demonstrating that PCL can induce mild membrane stress. Nevertheless, the levels remained below the 20% cytotoxicity threshold. Although slight variations occurred near the 80% threshold at higher doses, differences were not statistically significant and remained within acceptable biocompatibility limits for pulmonary polymeric systems. These findings demonstrate the potential of PCL nanoparticles to modulate RDV's cytotoxic profile, likely through controlled release mechanisms and reduced non-specific cellular interactions.

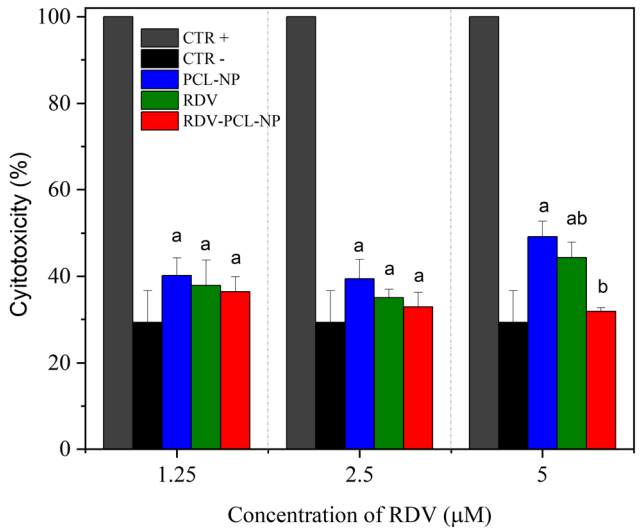

Fig. 3 Cytotoxicity analysis of remdesivir and the formulation containing or not RDV (RDV-PCL-NP and PCL-NP) performed on Vero E6 cells through the LDH assay. RDV concentrations (1.25, 2.50, and 5 μM) tested in the RDV formulation (RDV-PCL-NP), alongside Triton-X 1% (positive control). The values represent the mean ± standard deviation (SD) and correspond to data from two independent biological experiments, each conducted in triplicate. Different letters indicate statistical differences among columns at the same time ($p < 0.05$).

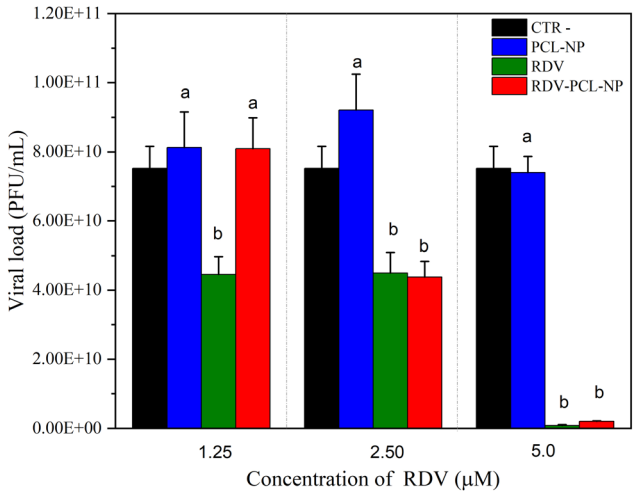

Fig. 4 Viral load measured in terms of PFU per mL in Vero E6 cells infected with SARS-CoV-2 and treated with remdesivir (RDV), RDV-PCL-NP formulation, and PCL-NP. Samples evaluated at three RDV concentrations: 1.25 μM, 2.50 μM, and 5 μM, considering an MOI = 1. The values represent the mean ± standard deviation (SD), derived from two independent biological experiments, performed in triplicate. Different letters indicate statistical differences among columns at the same time ($p < 0.05$).

Previous reports have highlighted the cytotoxic effects of RDV at higher concentrations due to its interference with mitochondrial polymerases and off-target host cell effects.[22] As revised by Farjadian *et al.* (2019), formulations containing PCL or PLGA-based nanoparticles are designed to enhance the therapeutic efficacy at low doses, thereby minimizing toxicity.[23] This focus is of paramount importance, as a concentration of up to 2.5 μM has been shown to be sufficient to achieve the desired therapeutic effect without compromising cell viability.[24]

3.3 Viral load analysis

The antiviral efficacy of free RDV and RDV-loaded polycaprolactone nanoparticles (RDV-PCL-NP) was assessed by quantifying viral load (PFU per mL) after RDV treatment at concentrations of 1.25, 2.5, and 5 μM. The untreated negative control (CTR−) and placebo nanoparticles (PCL-NP) showed high viral loads (~10^{10}–10^{11} PFU per mL) at all tested concentrations, confirming the absence of antiviral activity under these conditions (Fig. 4).

At 1.25 μM, free RDV reduced viral load compared to CTR−, suggesting an antiviral effect. However, at 2.5 μM both free RDV and RDV-PCL-NP achieved a marked reduction in viral load compared to CTR− ($p < 0.05$), highlighting a dose-dependent antiviral response. At the threshold dose of 5 μM, both free RDV and RDV-PCL-NPs exhibited comparable antiviral activity, suggesting that the pronounced effect observed at this concentration may be related to a saturation threshold rather than an intrinsic enhancement of efficacy by the nanoparticulate delivery system. However, at lower concentrations, differences in cellular uptake and release kinetics may still contribute to the enhanced performance of the encapsulated formulation.[25]

3.4 Preparation of the polymeric nano-in-microparticle powder formulation (RDV-PCL-MP)

The optimization of the spray-drying process parameters, including an inlet temperature of 100 °C, an outlet temperature of 64 °C, an aspiration flow of 70%, an atomization flow rate of 600 L h^{-1}, and a feed rate of 4.55 mL min^{-1}, resulted in the optimized powder formulation. The selected inlet and outlet temperatures maintained the PCL in the solid state, thereby preventing microparticle coalescence and preserving structural integrity throughout the drying process, while also preventing RDV degradation.[26] Furthermore, the addition of 1% w/w micronized lactose (LH206) as a drying adjuvant ensured the formulation stability, thereby yielding a homogeneous white powder.

Several factors influence the yield of the spray-drying process, including the nature of the material undergoing drying, the equipment operational parameters (for instance, inlet and outlet air temperatures, airflow, and feed rate), and the physicochemical properties of the product. In general, industrial spray-drying processes achieve yields ranging from 30% to 70%.[27] However, in the case of bench-scale spray-dryers, yields are generally found to be less than 70%. Here the final process yield was 63% for RDV-PCL-MP and 61% for PCL-MP. We understand that there is no need to present an encapsulation efficiency value for RDV-PCL-MP since we simply added 1% of lactose to the nanoformulation and removed the water content. Considering the lactose added, the RDV-PCL-MP drug loading (%DL) was estimated to be 0.96%.

The results obtained demonstrated the versatility of the encapsulation strategy by emulsion/diffusion/solvent evaporation combined with spray-drying. This supports the applicability of the strategy for other hydrophobic drugs within the framework proposed by our research group.[14]

3.5 Characterization of the RDV-PCL-MP inhalable powder

The comprehensive characterization of the formulated microparticles containing RDV and polymeric matrices was carried out through differential scanning calorimetry (DSC), thermogravimetric analysis (TGA), powder X-ray diffraction (PXRD), and Fourier-transform infrared spectroscopy (FTIR) (Fig. 5).

3.5.1 Thermal behavior: DSC and TGA. The DSC thermograms revealed distinct thermal transitions corresponding to the different components in the formulation (Fig. 5a). Pure RDV demonstrated an endothermic peak at approximately 140.7 °C, indicative of its melting point. In contrast, the formulated microparticles demonstrated a shift or broadening of this peak, indicating molecular dispersion within the polymeric matrix.[26] The presence of PCL, DPPC, and other excipients is likely to have contributed to this shift, suggesting weak interactions between the drug and excipients.[28]

TG analysis offered insights into the thermal stability of the formulations (Fig. 5b). RDV exhibited a weight loss event at 193.1 °C, corresponding to its initial thermal degradation. These findings are in close alignment with those reported by Bakhei *et al.* (2023), who observed the onset of RDV degradation at approximately 200 °C.[29] The formulation RDV-PCL-MP demonstrated enhanced thermal stability, with degradation occurring at a higher temperature (350 °C). This finding indicates that encapsulation within the polymeric matrix protects RDV from premature degradation, which is crucial to maintain drug integrity during storage and processing.

3.5.2 Crystallinity assessment: PXRD analysis. X-ray diffraction patterns confirmed the changes in crystallinity induced by encapsulation (Fig. 5c). RDV exhibited sharp and intense peaks at 16.32° and 22.36° (2θ), accompanied by lower-intensity peaks at 12.82°, 17.08°, and 24.48° (2θ). These observations are indicative of its crystalline nature.[29,30] These peaks were markedly reduced in intensity or even absent in the RDV-PCL-MP, indicating a decrease in crystallinity. It is important to highlight that reduction of peak intensity may reflect a decrease in the size of the crystallite rather than reflect a complete amorphization. Reduced crystallinity can enhance the drug solubility and bioavailability of RDV. On the other hand,

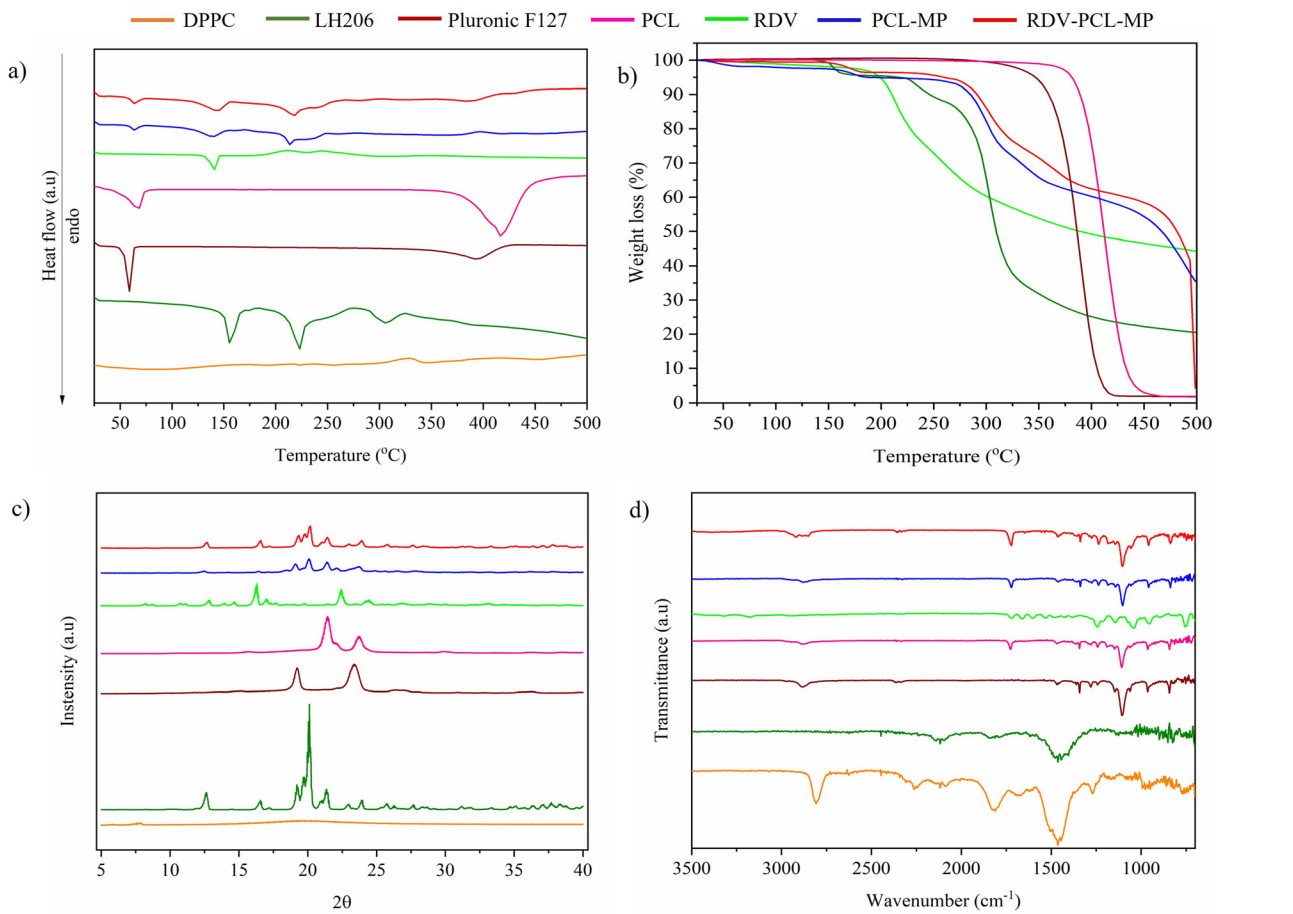

Fig. 5 (a) DSC, (b) TG, (c) DRX, and (d) FTIR, illustrating the thermal transitions, stability, crystallinity and molecular interaction of excipients: DPPC, LH206, Pluronic F127, RDV and formulations containing or not RDV: PCL-MP and RDV-PCL.

an amorphous phase may recrystallize over time, potentially compromising the formulation's stability and therapeutic performance.[31,32]

3.5.3 Molecular interactions: FTIR spectroscopy. FTIR spectroscopy was employed to assess the possible chemical interactions between RDV and the excipients (Fig. 5d). The spectra of pure RDV exhibited characteristic absorption bands at 1713 cm^{-1}, 2500–3400 cm^{-1}, and 3300–3500 cm^{-1}, corresponding to the functional groups carbonyl (C═O), hydroxyl (–OH), and amine (–NH).[33] Upon encapsulation (RDV-PCL-MP), shifts or changes in the intensity of these bands were observed, particularly in the C═O stretching and N–H bending regions. These alterations indicate potential hydrogen bonding or molecular interactions between RDV and the polymeric matrix, further supporting the hypothesis of successful encapsulation and improved physicochemical stability.[29]

It is evident from the correlation of data from DSC, TG, PXRD, and FTIR that the microparticle formulations successfully encapsulated RDV, modifying its physicochemical properties to improve stability. The reduction in crystallinity observed in DRX, in conjunction with the DSC and FTIR findings, supports the hypothesis that crystallinity of RDV is lower within the polymeric system. Moreover, the TG analysis corroborates the enhanced thermal stability.

3.5.4 Particle size distribution. The particle size distribution of the PCL-MP and RDV-PCL-MP formulations is presented in Fig. 6. Both formulations exhibited particle sizes ranging from 0.918 μm to 4.878 μm, with low polydispersity (span $\leq$ 2), a property that is critical for ensuring accurate dosing.[34] Specifically, RDV-PCL-MP presented $D(0.10)$ = 1.202 ± 0.059 μm, $D(0.50)$ = 2.360 ± 0.015 μm, and $D(0.90)$ = 4.111 ± 0.712 μm (Table 1). This finding aligns with the observation that particles within the 1–5 μm range are ideal for reaching the alveolar regions of the lungs.[35] PCL microparticles encapsulating drugs such as paclitaxel, doxorubicin, ibuprofen, and azithromycin have been previously investigated[14,34,36,37] and particle size ranges of 1–5 μm, 2–6 μm, 1–4 μm, and 1–5 μm in diameter, respectively, were reported.

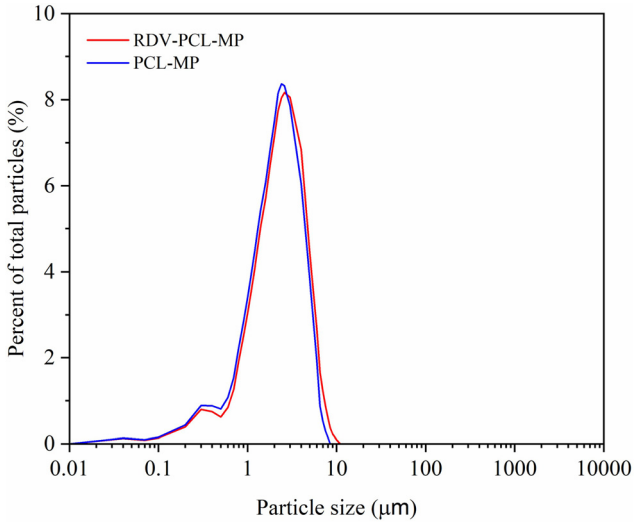

Fig. 6 Particle size distribution by laser diffraction of spray-dried PCL-MP and RDV-PCL-MP formulations.

Table 1 Particle size distribution of RDV-PCL-MP and PCL-MP formulations

Formulation	D (0.1) (μm)	D (0.5) (μm)	D (0.9) (μm)	Span
RDV-PCL-MP	1.20 ± 0.06	2.36 ± 0.02	4.11 ± 0.71	1.63
PCL-MP	0.92 ± 0.01	2.59 ± 0.03	4.88 ± 0.53	1.78

3.5.5 Particle morphology. The microscopic images of LH206 lactose and the formulations are presented in Fig. 7. As demonstrated in Fig. 7a, lactose consists of spherical particles with a diameter of less than 5 μm and exhibits highly porous surfaces. This outcome was expected since concentrations lower than 1% have been shown to result in the formation of more porous particles due to the rapid evaporation of water that creates spaces within the particles, thereby increasing porosity.[38] Fig. 7b corresponds to the micrograph of the blank formulation (PCL-MP) and presents particles ranging from 1 to 5 μm. Fig. 7c and d, corresponding to the RDV-PCL-MP formulation at 2500× and 10 000× magnification, respectively, reveal irregularly shaped structures. These characteristics are ascribed to the process of spray-drying, given that variations in solvent evaporation rates and processing conditions influence the morphology of the resulting particles. Furthermore, the particles demonstrate surfaces that are both rough and porous. This is likely a consequence of solvent evaporation during nanoparticle preparation, inducing the formation of pores. Porous microparticles offer several advantages, including an increased surface area that enhances solubility, improves drug bioavailability, facilitates penetration into the alveolar regions of the lungs, and reduces airway irritation.[39] The particles exhibit elongated and spherical shapes, proper powder dispersion, and a small particle size (1–5 μm), which may contribute to a desirable drug delivery to the airways.[40]

3.5.6 Aerodynamic performance by NGI. As Wong *et al.* (2023) pointede out, aerosolized particle size distribution and estimation of the fraction of particles reaching the target regions of the respiratory tract are essential to characterize inhalable powders.[30] In the present study, RDV-PCL-MP was aerosolized using the Next Generation Impactor (NGI), with the resultant particle deposition being observed at all stages of the impactor. The MMAD is a critical parameter that is assessed using the NGI, as it directly correlates with the ability of particles to reach the lower respiratory tract. According to Table 2, the MMAD of RDV-PCL-MP was determined to be 4.08 μm, adequate for deposition in the lower airways, including the bronchi and alveoli. Similar results were described in a previous work describing liposomal RDV nanoparticles in which the MMAD was 4.11 μm.[41] According to Zhang *et al.* (2010), particles within this size range are more likely to bypass the upper airway barriers (nasal cavity and throat) and reach the lungs, which is essential for treating viral respiratory diseases.[42]

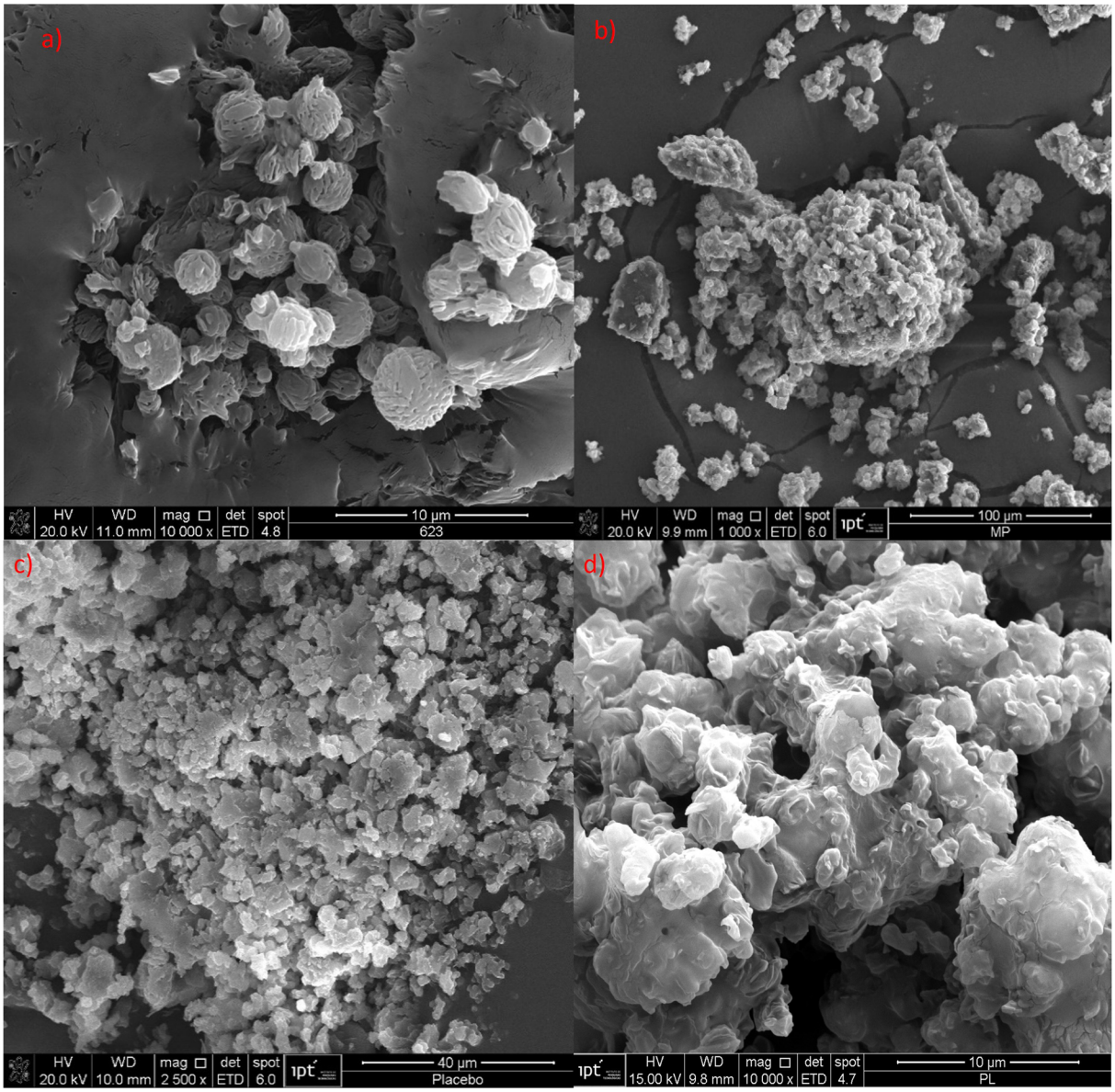

Fig. 7 Scanning electron micrography images of powders obtained after the spray-drying process: (a) LH206 lactose (10 000× magnification), (b) PCL-MP (1000× magnification), (c) RDV-PCL-MP (2500× magnification), and (d) RDV-PCL-MP (10 000× magnification).

Table 2 Aerodynamic properties of RDV-PCL-MPs determined by the next-generation impactor (NGI), including emitted dose (ED, %), fine particle fraction (FPF, %), respirable fraction (RF, %) and mass median aerodynamic diameter (MMAD, µm)

Formulation	ED (%)	FPF (%)	RF (%)	MMAD (µm)
RDV-PCL-MP	85	40	39	4.08

The ED% was found to be 85%, indicating that this percentage of the total drug is released from the inhalation device and is available for patient inhalation, ensuring effective pulmonary delivery. A similar result was found in other work, in which 87% of emitted dose was obtained by using other polymers such as PLGA and chitosan.[10] The FPF% was estimated to be 40%; it denotes the proportion of the emitted dose consisting of particles with an aerodynamic diameter below 5 µm. A respirable fraction of RF% was obtained, corresponding to 39% of the emitted dose. This fraction consists of particles between 1 and 5 µm in size, which are suitable for deposition in the lung.[43]

Previous work[10,44] demonstrated good aerodynamic properties of nano-in-microparticles containing RDV and acceptable lung deposition; however they lacked comprehensive antiviral efficacy studies and advanced characterization. In contrast, our work not only demonstrates efficient pulmonary deposition (*in vitro*) and high encapsulation efficiency, but also confirms antiviral activity against SARS-CoV-2 and formulation stability. In addition, compared to previously described nanoparticles of PCL and Pluronic

for RDV delivery,[44] the nano-in-micro particles produced here contain DPPC as a biocompatible stabilizer and lactose, providing a more robust polymeric matrix for nanoparticles and representing the most promising strategy.

4 Conclusions

In this study, an innovative polymeric nano-in-microparticle system (RDV-PCL-MP) was successfully developed and characterized for the purpose of pulmonary delivery of RDV. Considering that the usual IV administration of RDV results in rapid plasma elimination and limited pulmonary tissue distribution, this formulation offers a targeted approach for treating respiratory viral infections, including SARS-CoV-2. The combination of polycaprolactone (PCL) and lactose resulted in a dry powder formulation with ideal aerodynamic properties for deep lung deposition. Physicochemical analyses of the powder formulation confirmed the stability, homogeneity, and optimal particle size distribution within 1–5 μm, which is ideal for reaching the alveolar regions of the lungs where drug absorption is the most efficient. The high values of FPF% (40%) and RF% (39%) indicated the possibility of increased lung deposition. Furthermore, *in vitro* assays have demonstrated the nanostructures' effectiveness in reducing SARS-CoV-2 viral loads, with results comparable to those observed with the free drug. It is recommended that future studies concentrate on *in vivo* evaluations, long-term stability, and clinical trials to validate the safety and efficacy of the treatment in patients. This approach offers a transformative pathway for the localized treatment of viral infections, contributing to global health efforts against pandemics.

Author contributions

A. S.: conceptualization, methodology, data analyses, and writing – original draft; B. L.: viral assays' interpretation and data curation; B. R.: viral assays' interpretation and data curation; M. S.: next generation impactor test and data curation; M. C.: next generation impactor test and data curation; H. R.: formal analysis; N. C.: editing and reviewing; M. Z.: formal analysis, editing, and reviewing; J. M.: viral loading writing; V. A. F.: conceptualization, methodology, editing, and reviewing; C. Y.: formal analysis, editing, reviewing, project administration and supervision.

Conflicts of interest

The authors declare no conflict of interest.

Data availability

The data included in this article will be available on request to the corresponding authors.

Acknowledgements

Financial support from CAPES (88887.506666/2020-00) is acknowledged. We thank Lipid Ingredients (Brazil) and DFE Pharma (Germany) for donating the soybean lecithin S75® and the lactose, respectively. We are also very grateful to the scientific contributions made by Dr Patrícia Léo (*in memorian*).

References

1 P. O. Godwin, B. Polsonetti, M. F. Caron and T. F. Oppelt, Remdesivir for the Treatment of COVID-19: A Narrative Review, *Infect. Dis. Ther.*, 2024, **13**(1), 1–19.
2 J. J. Malin, I. Suárez, V. Priesner, G. Fätkenheuer and J. Rybniker, Remdesivir against COVID-19 and other viral diseases, *Clin. Microbiol. Rev.*, 2021, **34**(1), 1–21.
3 Y. Yasuda, Y. Hirayama, K. Uemasu, S. Arasawa, D. Iwashima and K.-i. Takahashi, Efficacy of the combination of baricitinib, remdesivir, and dexamethasone in hypoxic adults with COVID-19: A retrospective study, *Respir. Med. Res.*, 2022, **81**, 100903.
4 M. D. Waters and S. G. Warren, A tale of two drugs: Molnupiravir and Paxlovid, *Mutat. Res., Rev. Mutat. Res.*, 2025, **795**, 108533.
5 C. W. Chen, C. P. Chang, Y. S. Wen, C. H. Kuo, S. W. Lin, J. C. Tsai, *et al.*, Pulmonary delivery of remdesivir and dexamethasone encapsulated nanostructured lipid carriers for enhanced inflammatory suppression in lung, *J. Drug Delivery Sci. Technol.*, 2023, **90**, 105144.
6 I. Bulduk and E. Akbel, A comparative study of HPLC and UV spectrophotometric methods for remdesivir quantification in pharmaceutical formulations, *J. Taibah Univ. Sci.*, 2021, **15**(1), 507–513.
7 J. D. Goldman, D. C. B. Lye, D. S. Hui, K. M. Marks, R. Bruno, R. Montejano, *et al.*, Remdesivir for 5 or 10 Days in Patients with Severe Covid-19, *N. Engl. J. Med.*, 2020, **383**(19), 1827–1837.
8 H. W. Chan, H. W. Lee, S. Chow, D. C. L. Lam and S. F. Chow, Integrated continuous manufacturing of inhalable remdesivir nanoagglomerate dry powders: Design, optimization and therapeutic potential for respiratory viral infections, *Int. J. Pharm.*, 2023, **644**, 123303.
9 V. Sanna, S. Satta, T. Hsiai and M. Sechi, *Development of targeted nanoparticles loaded with antiviral drugs for SARS-CoV-2 inhibition*, 2022, p. 20.
10 V. Vijayan, S. Ravindran and A. Sockalingam, Dry Powder Inhaler Formulation of Remdesivir Mucoadhesive Nanoparticle for Respiratory Diseases, *J. Young Pharm.*, 2024, **16**(4), 753–761.
11 X. Li, S. Chang, G. Du, Y. Li, J. Gong, M. Yang, *et al.*, Encapsulation of azithromycin into polymeric microspheres by reduced pressure-solvent evaporation method, *Int. J. Pharm.*, 2012, **433**(1–2), 79–88.
12 M. Hoffman, H. Kleine-Weber, S. Schroeder, N. Kruger, T. Herrler, S. Erichsen, T. S. Schiergens, G. Herrler,

N. H. Wu, A. Nitsche, M. A. Muller, C. Drosten and S. Pohlmann, SARS-Cov-2 cell entry depends on ACE2 and TMPRSS2 and is blocked by a clinically proven protease inhibitor, *Cell*, 2020, **181**(2), 271–280e8.

13 V. M. Corman, O. Landt, M. Kaiser, R. Molenkamp, A. Meijer, D. K. W. Chu, *et al.*, Detection of 2019 novel coronavirus (2019-nCoV) by real-time RT-PCR, *Eurosurveillance*, 2020, **25**(3), 2000045.

14 A. T. Madrid Sani, K. L. V. Ramos-Rocha, M. A. Sarcinelli, M. H. da C. Chaves, H. V. A. Rocha, P. Léo, *et al.*, Development of a dry powder formulation for pulmonary delivery of azithromycin-loaded nanoparticles, *J. Pharm. Pharm. Sci.*, 2024, **27**, 1–15.

15 Z. Ma, L. Milton-mcgurk, P. Tang, H. K. Chan, D. Farina, S. Cheng, *et al.*, An experimental study of the effect of individual upper airway anatomical features on the deposition of dry powder inhaler formulations, *J. Aerosol Sci.*, 2024, **177**, 106320.

16 D. Quintanar-Guerrero, E. Allémann, H. Fessi and E. Doelker, Preparation techniques and mechanisms of formation of biodegradable nanoparticles from preformed polymers, *Drug Dev. Ind. Pharm.*, 1998, **24**(12), 1113–1128.

17 A. M. Pineda-Reyes, M. Hernández Delgado, M. De La Luz Zambrano-Zaragoza, G. Leyva-Gómez, N. Mendoza-Muñoz and D. Quintanar-Guerrero, Implementation of the emulsification-diffusion method by solvent displacement for polystyrene nanoparticles prepared from recycled material, *RSC Adv.*, 2021, **11**(4), 2226–2234.

18 M. Chakravarty and A. Vora, Nanotechnology-based antiviral therapeutics, *Drug Delivery Transl. Res.*, 2021, **11**(3), 748–787.

19 K. S. Soppimath, T. M. Aminabhavi, A. R. Anandro and W. E. Rudzinski, Biodegradable polymeric nanoparticles as drug delivery devices, *J. Controlled Release*, 2001, **70**, 1–20.

20 E. Halevas, B. Mavroidi, C. Kokotidou, G. Litsardakis and M. Pelecanou, Remdesivir-loaded bis-MPA hyperbranched dendritic nanocarriers for pulmonary delivery, *J. Drug. Deliv. Sci. Technol.*, 2022, 6, DOI: 10.1016/j.jddst.2022.103625.

21 I. J. Ferreira, L. R. de Menezes and M. I. B. Tavares, Obtaining PCL/tea tree oil particles with antimicrobial capacity and high cytocompatibility, *Polym. Bull.*, 2024, **81**(17), 15995–16020.

22 C. J. Gordon, E. P. Tchesnokov, J. Y. Feng, D. P. Porter and M. Götte, The antiviral compound remdesivir potently inhibits RNAdependent RNA polymerase from Middle East respiratory syndrome coronavirus, *J. Biol. Chem.*, 2020, **295**(15), 4773–4779.

23 F. Farjadian, A. Ghasemi, O. Gohari, A. Roointan, M. Karimi and M. R. Hamblin, Nanopharmaceuticals and nanomedicines currently on the market: Challenges and opportunities, *Nanomedicine*, 2019, **14**, 93–126.

24 S. Sharma, R. Parveen and B. P. Chatterji, Toxicology of Nanoparticles in Drug Delivery, *Curr. Pathobiol. Rep.*, 2021, **9**(4), 133–144.

25 H. K. Makadia and S. J. Siegel, Poly Lactic-co-Glycolic Acid (PLGA) as biodegradable controlled drug delivery carrier, *Polymers*, 2011, **3**(3), 1377–1397.

26 Y. A. Haggag and A. M. Faheem, Evaluation of nano spray drying as a method for drying and formulation of therapeutic peptides and proteins, *Front. Pharmacol.*, 2015, **6**(JUL), 1–5.

27 P. Sundararajan, J. Moser, L. Williams, T. Chiang, C. Riordan, M. Metzger, *et al.*, Driving Spray Drying towards Better Yield: Tackling a Problem That Sticks Around, *Pharmaceutics*, 2023, **15**(8), 3–6.

28 O. Sánchez-Aguinagalde, E. Meaurio, A. Lejardi and J. R. Sarasua, Amorphous solid dispersions in poly(ε-caprolactone)/xanthohumol bioactive blends: Physicochemical and mechanical characterization, *J. Mater. Chem. B*, 2021, **9**(20), 4219–4229.

29 A. H. Bakheit, H. Darwish, I. A. Darwish and A. I. Al-Ghusn, Remdesivir, *Profiles Drug Subst., Excipients, Relat. Methodol.*, 2023, **48**, 71–108.

30 S. N. Wong, K. H. Low, Y. L. Poon, H. W. Chan and S. F. Chow, Synthesis of the first remdesivir cocrystal: design, characterization, and therapeutic potential for pulmonary delivery, *Int. J. Pharm.*, 2023, **640**, 122983.

31 S. Drescher and P. van Hoogevest, The phospholipid research center: Current research in phospholipids and their use in drug delivery, *Pharmaceutics*, 2020, **12**(12), 1–36.

32 D. S. Kohane and R. Langer, Biocompatibility and drug delivery systems, *Chem. Sci.*, 2010, **1**(4), 441–446.

33 N. Krisanova, N. Pozdnyakova, A. P. Dudarenko, O. Shatursky, O. Gnatyuk, U. Afonina, *et al.*, Amphiphilic anti-SARS-CoV-2 drug remdesivir incorporates into the lipid bilayer and nerve terminal membranes influencing excitatory and inhibitory neurotransmission, *Biochim. Biophys. Acta, Biomembr.*, 2022, **1864**(8), 183945.

34 P. Party, D. Kókai, K. Burián, A. Nagy, B. Hopp and R. Ambrus, Development of extra-fine particles containing nanosized meloxicam for deep pulmonary delivery: In vitro aerodynamic and cell line measurements, *Eur. J. Pharm. Sci.*, 2022, **176**(1), 106247.

35 E. Dimbath, V. Maddipati, J. Stahl, K. Sewell, Z. Domire, S. George, *et al.*, Implications of microscale lung damage for COVID-19 pulmonary ventilation dynamics: A narrative review, *Life Sci.*, 2021, **274**, 119341.

36 A. Fahmi, M. A. Rahman, O. Mahareek and A. Mohamed, Synthesis, characterization, and cytotoxicity of doxorubicin - loaded polycaprolactone nanocapsules as controlled anti - hepatocellular carcinoma drug release system, *BMC Chem.*, 2022, 1–15, DOI: 10.1186/s13065-022-00888-w.

37 G. V. Salmoria, F. Sibilia and V. G. Henschel, Structure and properties of polycaprolactone/ibuprofen rods prepared by melt extrusion for implantable drug delivery, *Polym. Bull.*, 2017, **74**(12), 4973–4987.

38 J. Moser, *Spray Drying Technol.*, 2010, **1**, 1–46.

39 S. Mangal, R. Xu, H. Park, D. Zemlyanov, N. Shetty, Y. W. Lin, *et al.*, Understanding the Impacts of Surface Compositions on the *In vitro* Dissolution and Aerosolization of Co-Spray-Dried Composite Powder Formulations for Inhalation, *Pharm. Res.*, 2019, **36**(1), 6, DOI: 10.1007/s11095-018-2527-x.

40 K. Knap, K. Kwiecien, K. Reczynska-Kolman and E. Pamula, Inhalable microparticles as drug delivery systems to the lungs in a dry powder formulations, *Regener. Biomater.*, 2023, **10**, rbac099.

41 J. Li, K. Zhang, D. Wu, L. Ren, X. Chu, C. Qin, *et al.*, Liposomal remdesivir inhalation solution for targeted lung delivery as a novel therapeutic approach for COVID-19, *Asian J. Pharm. Sci.*, 2021, **16**(6), 772–783.

42 Y. Zhang, X. Wang, X. Lin, X. Liu, B. Tian and X. Tang, High azithromycin loading powders for inhalation and their in vivo evaluation in rats, *Int. J. Pharm.*, 2010, **395**(1–2), 205–214.

43 T. Saha, S. Sinha, M. Quinonez-Mateu and S. C. Das, Inhalable dry powder containing remdesivir and disulfiram: Preparation and in vitro characterization, *Int. J. Pharm.*, 2023, **645**, 123411.

44 S. A. Fouad, F. A. Malaak, M. H. Teaima, S. Omar, O. Kutkat, S. F. Elhabal, *et al.*, Novel inhalable nano-based/microparticles for enhanced sustained pulmonary delivery of remdesivir - A patient malleable treatment for coronaviruses infection: In vitro aerosolization, cytotoxicity assays and antiviral activity studies, *J. Drug Delivery Sci. Technol.*, 2024, **101**(PA), 106196.